Published in final edited form as:
Circulation. 2013 September 17; 128(12): . doi:10.1161/CIRCULATIONAHA.113.003072.

TGF-β Signaling Promotes Pulmonary Hypertension Caused by *Schistosoma Mansoni*

Brian B. Graham, MD[1,2], **Jacob Chabon, BS**[1], **Liya Gebreab**[1], **Jennifer Poole, BS**[1], **Elias Debella**[1], **Laura Davis, BS**[1], **Takeshi Tanaka, MD**[1], **Linda Sanders, BS**[1], **Nina Dropcho**[1], **Angela Bandeira, MD**[2,3], **R. William Vandivier, MD**[1], **Hunter C. Champion, MD**[2,4], **Ghazwan Butrous, MD**[2,5], **Xiao-Jing Wang, MD**[6], **Thomas A. Wynn, PhD**[7], and **Rubin M. Tuder, MD**[1,2]

[1]Program in Translational Lung Research, Division of Pulmonary Sciences and Critical Care Medicine, Anschutz Medical Campus, Aurora, CO

[2]Pulmonary Vascular Research Institute, Recife, Brasil

[3]Memorial S. Jose Hospital, Universidade de Pernambuco in Recife, Recife, Brasil

[4]Division of Cardiology, University of Pittsburgh

[5]School of Pharmacy, University of Kent, Kent, UK

[6]Department of Pathology, Anschutz Medical Campus, Aurora, CO

[7]Immunopathogenesis Section, Laboratory of Parasitic Diseases, NIAID, NIH

Abstract

Background—The pathogenic mechanisms underlying pulmonary arterial hypertension (PAH) due to schistosomiasis, one of the most common causes of pulmonary hypertension (PH) worldwide, remains unknown. We hypothesized that TGF-β signaling as a consequence of Th2 inflammation is critical for the pathogenesis of this disease.

Methods and Results—Mice sensitized and subsequently challenged with *S. mansoni* eggs developed PH associated with an increase in right ventricular systolic pressure (RVSP), thickening of the pulmonary artery media, and right ventricular hypertrophy. Rho-kinase dependent vasoconstriction accounted for about 60% of the increase in RVSP. The pulmonary vascular remodeling and PH were dependent on increased TGF-β signaling, as pharmacological blockade of the TGF-β ligand and receptor, and mice lacking Smad3 were significantly protected from *Schistosoma*-induced PH. Blockade of TGF-β signaling also led to a decrease in IL4 and IL13 concentrations, which drive the Th2 responses characteristic of schistosomiasis lung pathology. Lungs of patients with schistosomiasis-associated PAH have evidence of TGF-β signaling in their remodeled pulmonary arteries.

Conclusions—Experimental *S. mansoni*-induced pulmonary vascular disease relies on canonical TGF-β signaling.

Correspondence: Brian B. Graham, MD, Division of Pulmonary Sciences and Critical Care Medicine, University of Colorado Denver 12700 East 19th Avenue, C-272, Aurora, CO 80045, Phone: 303 724 3876, Fax: 303 724 6042, brian.graham@ucdenver.edu.

Conflict of Interest Disclosures: None.

Keywords

schistosomiasis; pulmonary hypertension; TGF-beta

Introduction

Pulmonary hypertension is a significant cause of morbidity and mortality in the developing world, largely due to schistosomiasis or chronic high altitude exposure, together affecting approximately 1 in 350 individuals[1]. The trematode *Schistosoma* is the third most common parasitic infection worldwide, affecting over 200 million people; approximately 6.1% of individuals with recurrent chronic infection develop pulmonary arterial hypertension (PAH)[2]. Pathologically, pulmonary vascular disease due to schistosomiasis shares the pulmonary vascular histopathology of other forms of WHO group 1 PAH, including idiopathic PAH (IPAH) and connective tissue disease-associated PAH (CTD-PH)[3,4]. This remodeling includes thickening of the media, neoplastic-like proliferation of endothelial cells in the intima, and inflammatory infiltrates in the adventitia. The shared pulmonary vascular remodeling in PAH suggests that, despite differences in etiology, common aspects of pathogenesis promote schistosomiasis-induced PAH, IPAH and CTD-PAH. Insights into the pathogenesis of schistosomiasis-induced PAH thus may not only have profound impact on the disease worldwide but also instruct the clinical management of PAH as whole.

The most prevalent species and the one particularly associated with PAH is *S. mansoni*. *Schistosoma* have an obligate 2 host lifecycle: the snail intermediate host releases cercariae into water, which penetrates the skin of susceptible animals (humans, mice and birds for example). After infecting individuals, the parasites mate in the vasculature of the gastrointestinal tract, releasing eggs that reach the intestinal lumen. A large percentage of the eggs are retained within the host, many of which are carried via the portal venous system into the portal triads. The initial reaction to *Schistosoma* is Th1 dominated, due to worm-derived antigens, with eosinophils and neutrophils secreting TNF-α, IL1, IL6, and IFN-γ[5,6]. The chronic infection is characterized by Th2 inflammation, primarily directed against egg-derived antigens; in this context cytokines including IL4, IL5, IL10 and IL13 drive the formation of granulomas containing lymphocytes, fibrocytes and macrophages[7]. Once induced by Th2-CD4+ T-cells, macrophages stimulated by *Schistosoma* infection become alternatively activated (M2 phenotype).

We hypothesized that TGF-β signaling is necessary for the pathogenesis of experimental pulmonary hypertension (PH) due to *Schistosoma*. We employed pharmacological blockade of TGF-β signaling and mice lacking the canonical intracellular TGF-β signaling molecules Smad2 and/or Smad3 exposed to *S. mansoni*, and validated our findings with human tissue collected at autopsy from individuals who died of schistosomiasis associated-PAH. In contrast to the lack of a pathogenic role of TGF-β in hepatic *Schistosoma* inflammation and fibrosis[8], our study documents that TGF-β signaling is involved in PH in mice and possibly humans resulting from exposure to *S. mansoni* antigens.

Methods

Animals

Smad2+/− and Smad3+/− on an ICR × B129 background were provided by Chuxia Deng, NIH. RELM-α −/− mice on a Balb-c background were provided by Regeneron Pharmaceuticals (Tarrytown, NY). The phenotypes of these transgenic models have been previously described(9–11). Because of the complex background of these genotypes, wildtype littermates were used as controls. Wildtype C57Bl6/J mice (and Balb-c mice to

serve as controls to RELM-α −/− mice) were purchased (Taconic, Hudson, NY). All experimental procedures in rodents were approved by the Animal Care and Use Committees at the University of Colorado Denver.

Treatments

S. mansoni eggs were obtained from homogenized and purified livers of Swiss-Webster mice infected with cercariae, provided by the Biomedical Research Institute (Rockville, MD). Experimental mice were intraperitoneally and intravenously challenged with *S. mansoni* eggs at the timepoints indicated, at a dose of 240 eggs/gram body weight. SB431542 (Sigma-Aldrich, St. Louis, MO), LY364947 (Sigma-Aldrich), and SB203580 (LCLabs, Woburn, MA) was purchased, reconstituted in DMSO, diluted in PBS, and administered intraperitoneally at the timepoints indicated in the figures at the following doses: SB431542: 4.2μg/g/day; LY364947 1μg/g/day; SB203580: 20μg/g/day. Control mice received the same volume of DMSO diluted in PBS without the active drug. Monoclonal mouse anti-pan-TGF-β antibody (clone 1D11) was purchased from American Type Culture Collection (Manassas, VA) and grown in a bioreactor by the UCDenver Tissue Culture Core Facility. 1D11 or control IgG (R&D Systems, Minneapolis, MN) was administered IP at a dose of 0.5μg/g every 3 days, as indicated in the figures. Mice were placed in a hypoxia chamber and administered 10% FiO_2 for 3 weeks duration, controlled by an oxygen sensor feedback loop (Proox 110, BioSpherix, Lacona, NY).

Assessment of PH

Measurement of the right ventricular pressure was performed as previously described[9]. Mice were anesthetized with ketamine/xylazine and ventilated through a transtracheal catheter. The abdominal and thoracic cavities were opened, and a 1Fr pressure-volume catheter (PVR-1035, Millar Instruments, Houston, TX) was placed through the right ventricle apex to transduce the pressure. Fasudil (LC Laboratories, Woburn, MA) was administered IV acutely 30mg/kg during RV pressure tracing and the post-treatment RVSP recorded 5 minutes later.

Protein and RNA Assessment

Immunostaining was performed on mouse and human tissue using the reagents in Supplemental Tables 1 and 2 respectively. Protein from mouse whole lung lysates was used for Western blot and ELISA with the reagents in Supplemental Tables 3 and 4 respectively. mRNA was retrieved from mouse whole lung tissue by Qiagen RNAeasy kit (Hilden, Germany). mRNA expression levels were quantified using an Illumina (San Diego, CA) HiSeq 2000 RNA sequencing (RNA-seq) system, and the reads mapped to the mouse NCBI Build 37/mm9 genome using CASAVA v1.7 (Illumina).

Statistics

Statistical analyses were performed in SigmaStat v2.03 (IBM, Armonk, NY). Data are presented as mean ± standard error. Differences between two groups were assessed using the rank-sum test and for three or more groups the Kruskal-Wallis test/analysis of variance on ranks followed by Dunn's post-hoc test. $P < 0.05$ was considered to be statistically significant.

Additional details are in the Supplemental Methods.

Results

Role of pulmonary vascular remodeling in *Schistosoma*-induced PH

We employed a mouse model of *Schistosoma*-induced pulmonary vascular disease, triggered by sequential sensitization with *S. mansoni* parasite egg antigens (by intraperitoneal injection) followed by intravenous challenge with *S. mansoni* eggs (delivered by tail vein injection). This protocol allowed us to employ a relevant mouse model while shortening the natural life cycle, which requires 2–3 months time for mature worms to deposit eggs that reach the liver and cause lung disease[9]. Indeed, our experimental protocol caused pulmonary interstitial and vascular disease as seen in the natural life cycle. Consistent with our prior observations, we confirmed that this mode of *Schistosoma* challenge leads to a significant increase in right ventricular systolic pressure (RVSP) and pulmonary artery media thickness (by both α-smooth muscle actin and smooth muscle myosin heavy chain staining), but not intima thickness in mice (denoted hereafter as Schisto-PH, Figures 1A–D and S1). The *S. mansoni*-exposed mice also developed a trend towards right ventricular hypertrophy (P=0.052) without significant fibrosis or myocyte hypertrophy (Figures 1E and S2). There were no differences in left ventricular systolic pressure, right or left ventricular diastolic pressures, heart rate, or body weight between *S. mansoni*-challenged and unchallenged mice (Figure S3).

We next sought to clarify the cause of the increased media thickness after *S. mansoni* egg exposure. Pulsing with intraperitoneally-injected BrdU early (3 days) or late (6 days) after IV egg augmentation allowed us to identify proliferating cells in the intima, media and adventitia of pulmonary arteries, particularly at early timepoints of vascular remodeling (Figures 2A–D). There was significant BrdU incorporation in cells surrounding egg-centered granulomas (Figures S4A–E). In both vessels and peri-egg granulomas BrdU+ cells co-localized with phospho-Smad2/3 nuclear activity, consistent with signaling due to TGF-β (Figures 2E and S4D and E), although the fraction of cells double-positive for Brdu and phospho-Smad2/3 among all BrdU+ cells did not significantly change with *S. mansoni* egg exposure (Figures S4F and G). A subpopulation of macrophages (Mac3+ cells) was also BrdU positive, indicative of macrophage proliferation *in situ* (Figure 2F)[10].

Bone marrow progenitors may contribute to the increased pulmonary vascular wall thickness in other forms of human PAH and experimental models of PH[11]. We interrogated for the presence of bone marrow-derived cells infiltrating the vasculature in Schisto-PH using mice with ubiquitous GFP+ bone marrow adoptively transferred into lethally irradiated wildtype recipient mice, which were then challenged with *S. mansoni*. Mice treated in this manner had significant GFP signal likely in inflammatory cells in the adventitia layer and peri-egg granulomas, but not in structural cells in the vascular intima or media (Figures 2G and S5). In aggregate, these data suggest that the lung inflammation caused by *S. mansoni* involves both recruitment of bone marrow cells and local cell proliferation.

Role of pulmonary vascular vasoconstriction in Schisto-PH

There is evidence that human schistosomiasis-associated PAH involves both pulmonary vasoconstriction and vascular remodeling(4,15). We sought to identify the selective contribution of the cellular components of pulmonary vascular remodeling and pulmonary artery vasoconstriction to the increase in RVSP observed in Schisto-PH. We found a 6-fold increase (P<0.05) in the concentration of activated (GTP-bound) RhoA, which has been implicated in pathologic vasoconstriction in other models of experimental PH(16), in whole lung lysates of mice exposed to *S. mansoni* as compared to unexposed mice (Figure 3A). Acute intravenous administration of fasudil, an inhibitor of Rho-activated kinase (ROCK), in *S. mansoni*-exposed mice resulted in a significant decrease in RVSP towards the baseline

pressures of unexposed mice 5 minutes after treatment, although the RVSP remained elevated post-fasudil administration compared to unexposed mice (*P*=0.052; representative RVSP tracings in Figure 3B; statistical analysis of the effect of fasudil in multiple mice in each group in Figures 3C and D). While the fasudil-treated mouse lungs showed persistent media thickening as in untreated Schisto-PH mice, the intima thickness was now also found to be significantly increased (Figures 3E and F), possibly due to thinning of the intima in control arteries after vasodilation.

A potential inducer of pulmonary vasoconstriction and Rho-ROCK activation is hypoxia, which might contribute to pulmonary vascular remodeling after *S. mansoni* egg exposure. We found that unanesthetized mice exposed to *S. mansoni* had normal tail oxygen saturation measured noninvasively (Figure S6A). Furthermore, intraperitoneal administration of pimonidazole hydrochloride (Hypoxyprobe) followed by staining for 2-nitroimidazole adducts to amino acid thiol groups (which occurs when the pO_2 is < 10mmHg[12]) failed to demonstrate significant tissue hypoxia in the pulmonary vasculature, while small regions of hypoxia were detected in the center of very large peri-egg granulomas (Figures S6B–G). Accordingly, we found no evidence of increased vascular hypoxia inducible factor (HIF)-1α activity as the expression of HIF-1α targets Glucose Transporter 1 (GLUT1) and Hexokinase 2 (HK2) were similar in *S. mansoni*-exposed mouse lung tissue when compared with the pulmonary vasculature of control mice (Figures S7 and S8). In line with these findings, no significant changes suggestive of increased Hif-1α activity in the pulmonary vascular compartment was observed for either of these proteins in the lung tissue of four subjects who died of schistosomiasis-associated PAH, as compared to two samples of control (unsuccessful donor) lung tissue. Specifically, 1 of the 4 subjects with schistosomiasis-associated PAH had an increase in intimal GLUT1, and 3 of the 4 subjects had decreased HK2 in the intima, and to a lesser extent decreased HK2 in the media as well, as compared to the control tissue (representative images are shown in Figures S9 and S10).

TGF-β signaling in *Schistosoma*-induced PH

Increased TGF-β family signaling has been implicated in multiple forms of human and experimental PH, including mice infected with *S. mansoni* and patients with schistosomiasis-associated PAH(12). We observed a significant (1.75-fold, *P<0.05)* increase in the levels of TGF-β1 mRNA as measured by RNA-seq in *S. mansoni*-exposed mice as compared to unexposed mice; there was no change in TGF-β2 or TGF-β3 expression with *S. mansoni* exposure (Figure 4A). The increase in TGF-β1 was dependent on the schistosomiasis-induced Th2 cytokines IL4 and IL13, as mice lacking both did not have increased TGF-β1 after *S. mansoni* exposure (Figure 4B).

Macrophages in the vascular adventitia potentially represented the main cellular source of TGF-β in mice infected with *S. mansoni*, based on immunodetection using a TGF-β1-specific antibody that preferentially binds active TGF-β1 (Figure 4C). Within the adventitia compartment, Mac3-positive area increased 4-fold, TGF-β1-positive area increased approximately 10-fold, and the cellular profiles positive for both Mac3 and TGF-β1 increased 8-fold after *S. mansoni* exposure (Figures 4D–F). Furthermore, the average pixel intensity of the anti-TGF-β1 stain within the adventitia increased 2-fold in all TGF-β1-positive areas (Figure 4H). Overall, 70% of the TGF-β1-positive area co-stained for Mac3, suggesting that the majority of TGF-β1 in the adventitia is produced by macrophages (Figure 4I). There was a similar increase in the Mac3, TGF-β1, and Mac3-TGF-β1 co-localizing areas as well as TGF-β1 intensity in both the lung parenchyma (excluding vessels and granulomas) and peri-egg granulomas after *S. mansoni* exposure (Figure S11).

We have previously documented increased TGF-β signaling in pulmonary arteries of mice exposed to *S. mansoni* and lungs of patients with schistosomiasis-associated PAH[9]. To

quantitatively complement these data, we observed a more extensive expression of phospho-Smad2/3 in the pulmonary vascular intima, media and adventitia regions in experimental Schisto-PH lungs when compared with control mice; moreover, the average intensity of the phospho-Smad2/3 stain was equally and significantly increased (about 1.5-fold) in all three pulmonary vascular compartments (Figure 5) as well as the lung parenchyma from infected mice (Figure S12). These changes are relevant to the human disease as we detected increased cellular profiles expressing phospho-Smad2/3 staining within the pulmonary vascular media compartment in subjects who died of this disease when compared with control human lungs (Figure 6).

Differential protection by inhibition of TGF-β and TGF-β signaling in Schisto-PH

To address whether TGF-β-induced signaling might contribute to the pathology of Schisto-PH, we tested the impact of neutralization of all TGF-β isoforms after *S. mansoni* exposure. Treatment with the anti-pan-TGF-β neutralizing antibody 1D11 resulted in partial protection against the increases in RVSP and media thickness induced by *S. mansoni* exposure (Figures 7A and B); no significant changes were seen in intima thickness, right ventricular hypertrophy, peri-egg granuloma volume, or clearance of eggs by the host (measured by quantifying the remaining egg burden after 4% KOH digest of the lung tissue) with 1D11 treatment (Figure S13).

Interleukins 4 and 13 (IL4 and IL13) are highly upregulated by *S. mansoni* infection, and activation of the Th2 immune response by an inhaled antigenic stimulus has been shown to induce pulmonary vascular remodeling[13]. We sought to determine if the prevention of PH by blocking the TGF-β signaling pathway after *S. mansoni* exposure correlated with decreases in IL4 and/or IL13. As anticipated, the amounts of IL4 and IL13 mRNA and protein were significantly increased after exposure to *S. mansoni* (Figures 7C–F). These increases trended towards suppression by treatment with 1D11. Taken together with our prior report of increased TGF-β signaling in schistosomiasis-infected mice lacking the decoy IL13 receptor IL13Rα2(12), these data indicate that IL4/IL13 and TGF-β form a mutually amplifying feedforward loop.

A potential mechanism for a decrease in IL4 and IL13 with TGF-β blockade would be a shift from a Th2 towards a Th1 immune response, which would be characterized by an increase in IFN-γ. However, we observed a mild (although significant) increase in IFN-γ RNA and protein levels after exposure to *S. mansoni*, which was not significantly altered by treatment with 1D11 or the TGF-β-R1 (ALK5) inhibitor SB431542 (Figure S14). We also investigated the IL4/IL13-target RELM-α, which has been reported to correlate with Th2-induced vascular remodeling(18,19). RELM-α mRNA and protein increased with *S. mansoni* exposure but were not modulated in mice protected by 1D11 (Figures S15A–C). Furthermore, RELM-α knockout mice were not protected against the increase in RVSP induced by *S. mansoni* exposure (Figure S15D).

We then tested the effect of blocking TGF-β-R1 (ALK5) kinase activity in *S. mansoni*-exposed mice using the two small molecule inhibitors SB431542 (which also blocks ALK4 and ALK7(20)) and LY364947 (which also blocks TGF-β-R2 and p38 MAP kinase(21)). Both of these inhibitors partially prevented the increase in RVSP induced by *S. mansoni* exposure (Figures 8A and B). Surprisingly, there was no significant effect on the increase in media thickness induced by *S. mansoni* exposure (Figures 8C and D). Similarly, there were no consistent trends in alterations in intima thickness, Fulton index, peri-egg granuloma volume, or the clearance of eggs by the host with either treatment, although the Fulton index was slightly increased with LY364947 treatment and egg clearance decreased with SB431542 treatment (Figure S16). These results suggest that the effectiveness of ALK5 blockade, particularly in regards to vascular remodeling, may be less than blockade at the

level of the TGF-β ligand, potentially due to incomplete ALK5 inhibition or non-ALK5 TGF-β receptor signaling (such as via ALK1).

We sought to characterize the individual roles of Smad2 and Smad3, which relay canonical intracellular TGF-β signaling, in *Schistosoma*-induced pulmonary vascular disease. We used Smad2+/−, Smad3+/−, Smad3−/− and Smad2+/−Smad3+/− (double heterozygous) mice; Smad2 homozygous deletion is embryonically lethal[14]. We found that Smad3−/− mice had a substantial protection against *Schistosoma*-induced PH (Figure 8E), although similar to the SB431542 and LY364947-treated mice, there was no effect by Smad3 deletion on the increase in medial thickness after *S. mansoni* exposure (Figure 8F). There was no significant benefit from Smad2+/−, Smad3+/−, or Smad2+/−Smad3+/− genotype, although there was a trend towards less medial remodeling in the Smad2+/− mice (Figures S17A and B). We then interrogated whether Smad3+/+ bone marrow transplantation into lethally ablated Smad3−/− recipients conferred sensitivity to pulmonary vascular disease due to *S. mansoni*. We observed that these mice were protected from *Schistosoma*-induced PH to a degree comparable to Smad3−/− mice (Figure 8E), suggesting that the relevant Smad3 signaling involved the non-bone marrow-derived cells, and potentially the components of the pulmonary vasculature. There were no consistent changes in intima thickness, Fulton index, peri-egg granuloma volumes, or the clearance of eggs by the host after *S. mansoni* egg exposure with these genetic modifications (Figures S17C–F).

We also studied the role of Smad signaling in a less inflammatory stimulus of PH, chronic hypoxia exposure. We found the Smad3+/− but not the Smad2+/− genotype was protected (at least partially) against chronic-hypoxia induced increase in RVSP by exposure to 3 weeks normobaric (Denver altitude) room air or 10% FiO_2, while neither genotype was significantly protected against the development of hypoxia-induced right ventricular hypertrophy (Figures S18A and B). Interestingly, we found that Smad2+/−Smad3+/− mice trended towards more severe disease than Smad2+/+Smad3+/− mice (Figure S18A), suggesting a protective role for Smad2 in chronic hypoxia exposure (Figures S18C and D).

We suspected that the decrease in RVSP in the setting of persistent medial thickness with TGF-β signaling blockade was accounted for by a vasodilation effect. Fasudil administration to Smad2+/−, Smad3+/− and Smad2+/−Smad3+/− mice after exposure to *S. mansoni* eggs led to reductions in RVSP comparable to wildtype mice (Figures 8G and S19). To test whether non-canonical TGF-β signaling mediated by p38 MAPK, implicated in models of familial (BMPR2 mutation) and hypoxic PH(22,23), may be relevant in Schisto-PH, we treated *Schistosoma*-exposed mice with the p38 MAPK inhibitor SB203580. We found inhibiting p38 MAPK had no effect on RVSP, degree of vasoconstriction as determined by response to fasudil treatment, media or intima remodeling, Fulton index, peri-egg granuloma volume, or egg clearance after *S. mansoni* egg-exposure (Figure S20).

Discussion

Our findings reveal a pathogenic role of TGF-β1 and Smad3-dependent TGF-β signaling in Schisto-PH. Reliant on neutralizing antibodies, pharmacologic blockade of TGF-β receptor signaling, and mice with a reduction in copy numbers of Smad2 and Smad3, we demonstrate that TGF-β contributes to *Schistosoma*-induced PH (Figure 8H). We found the Th2 cytokines IL4 and IL13 to be necessary for TGF-β activation; previously we observed IL13 gain-of-function to be sufficient for TGF-β activation(12). Coupled with the finding of IL4 and IL13 suppression by TGF-β signaling blockade, there may be a positive feedback loop of IL4/IL13 and TGF-β propagating the disease. Importantly, Schisto-PH does not represent a form of hypoxia-induced PH, as we found mice with this condition lacked peri- and intravascular hypoxia. The relevance of these experimental data are supported by

identification of TGF-β signaling in lungs of patients with Schisto-PAH, like that documented for IPAH and CTD-PAH[15]. The aggregate of these findings indicate that therapeutic targeting of TGF-β holds promise in the treatment of this highly prevalent disease.

A combination of portopulmonary hypertension and inflammation triggered by *Schistosoma* egg antigens likely contributes to PAH in patients infected with schistosomiasis(3). Pre-portal fibrosis resulting from chronic trematode infection and egg deposition can result in portal hypertension and porto-systemic shunts, facilitating embolization of *Schistosoma* ova to the lung. However, patients who currently die of schistosomiasis-associated PAH do not have a significant burden of intrapulmonary egg antigens(25), probably due to the modern widespread use of anti-helmenthics, often after egg translocation to the lungs. Thus, PAH resulting from schistosomiasis may result not only from egg embolization, but may be contributed by host response to localized deposition of egg antigens. Accordingly, we have experimentally observed that *Schistosoma*-induced PH requires intraperitoneal sensitization with egg antigens prior to intravenous egg augmentation, likely contributing to a robust Th2 immune response[9]. As demonstrated above, in the mouse hepatic disease is not required for Schisto-PH.

Our findings suggest a mechanistic link between the pathogenesis of schistosomiasis-associated PAH and other forms of WHO Group 1 PAH. Alterations in TGF-β family signaling have been implicated in heritable PAH from mutations in TGF-β family receptors including BMPR2, ALK1 and endoglin, leading to enhanced TGF-β induced growth in pulmonary artery smooth muscle cells; these findings complement the evidence of enhanced intracellular TGF-β signaling in idiopathic PAH[15,16]. However, no role for loss of BMPR2 in the development of pulmonary vascular disease due to *S. mansoni* has been detected in BMPR2 heterozygous mice[17]. In line with our findings, inhibition of TGF-β signaling also prevents experimental PH induced by hypoxia or exposure to the alkaloid toxin monocrotaline[18,19]. The *Schistosoma*-induced PH model therefore explicitly links host-induced inflammation and TGF-β with pulmonary vascular disease, which is likely relevant to the development of all forms of Group 1 PAH including IPAH and connective tissue disease-associated PAH[20].

We observed a Rho-kinase dependent vasoconstriction resulting in elevation in RVSP of about 30% in our mouse model of *Schistosoma*-induced PH, comparable to previously demonstrated rat models of PH[21,22]. Vasoreactivity is present in a subset of patients with schistosomiasis-associated PAH as well[23]. Even after fasudil treatment, we observed a significant increase in the thickness of the media and intima in mice exposed to *S. mansoni*. We found a disconnect between RVSP and the degree of vascular remodeling after blocking the TGF-β signaling pathway, in that mice had a substantial decrease in RVSP but only a borderline decrease in vascular remodeling with TGF-β1 ligand blockade and no change in vascular remodeling with inhibition of the ALK5 receptor or Smad2/3 loss of function. We suspected that much of the decrease in RVSP may be due to alterations in vascular tone, but treatment with the Rho kinase inhibitor fasudil did not reveal a difference in Rho kinase-mediated vasoconstriction after inhibition of TGF-β signaling. We did not observe a significant effect of TGF-β signaling blockade on the right ventricle as determined by right ventricular hypertrophy (Fulton index) or cardiac output (data not shown). Alternative causes for the greater decrease in RVSP than vascular remodeling may include signaling via ALK1, an effect on intima thickness (an increase in intima thickness was only seen after quantifying fasudil-treated mice), and/or non-Rho kinase-mediated vasoconstriction. It is also possible that the doses of the TGF-β signaling inhibitors used were inadequate to fully protect against *S. mansoni*-induced vascular remodeling, although effects on RVSP were

observed for all compounds, and the phenotype induced was comparable to genetic ablation of the canonical TGF-β signaling mediator Smad3.

Our studies interrogated for the first time the relative contributions of the canonical mediators Smad2 and Smad3 in PH. Smad2 and Smad3 have differential actions in cancers, with Smad2 suppressing tumor growth and Smad3 promoting tumor growth[24]. We found that in *Schistosoma*-induced PH, Smad3, specifically within the peripheral non-bone marrow-derived compartment, may be largely responsible for PH and may contribute to vascular remodeling. Of note, complete loss of Smad3 may be required based on protection seen in Smad3−/− mice when compared with the heterozygous mouse or the compounded Smad2+/−Smad3+/− mouse. In contrast the loss of a single copy of Smad3 partially protected against hypoxia-induced PH. We did not observe a significant effect of suppressing Smad2 in Schisto-PH or hypoxia-induced PH.

Despite the availability of effective single dose anti-helmenthics such as praziquantel[25], significant social and economic hurdles prevent adequate epidemiological control of Schistosoma, which is compounded by restricted access to available treatment and cultural hurdles to proper sanitation and exposure[26]. Given the worldwide burden of schistosomiasis-associated PAH, with potentially over 10 million affected individuals, elucidation of the disease pathogenesis remains a key to developing specific treatments. Thus, our study provides not only novel insights into the pathogenic role of TGF-β signaling in Schisto-PH but expands the scope of therapeutic targets. Interruption of the positive feedback interaction between IL4/IL13 and TGF-β signaling with biologicals targeted to the former[27] or Smad3 inhibitors to the latter may provide viable candidates to treat schistosomiasis-induced PAH.

Supplementary Material

Refer to Web version on PubMed Central for supplementary material.

Acknowledgments

Smad2+/− and Smad3+/− mice were provided by Chuxia Deng, NIH. RELM-α−/− mice were provided by Regeneron Pharmaceuticals.

Funding Sources: This study was supported by Parker B. Francis, NIH K08HL105536, and Pfizer Advancing Science through Pfizer Investigator-Research Exchange (ASPIRE) grants to BBG.

References

1. Butrous G, Ghofrani HA, Grimminger F. Pulmonary vascular disease in the developing world. Circulation. 2008; 118:1758–1766. [PubMed: 18936338]
2. Ward TJC, Fenwick A, Butrous G. The prevalence of pulmonary hypertension in schistosomiasis: a systematic review. PVRI Review. 2011; 3:12–21.
3. Graham BB, Bandeira AP, Morrell NW, Butrous G, Tuder RM. Schistosomiasis-associated pulmonary hypertension: pulmonary vascular disease: the global perspective. Chest. 2010; 137:20S–29S. [PubMed: 20522577]
4. Tuder RM. Pathology of pulmonary arterial hypertension. Semin Respir Crit Care Med. 2009; 30:376–385. [PubMed: 19634077]
5. Boros DL, Whitfield JR. Enhanced Th1 and dampened Th2 responses synergize to inhibit acute granulomatous and fibrotic responses in murine schistosomiasis mansoni. Infect Immun. 1999; 67:1187–1193. [PubMed: 10024559]
6. de Jesus AR, Silva A, Santana LB, Magalhaes A, de Jesus AA, de Almeida RP, Rego MA, Burattini MN, Pearce EJ, Carvalho EM. Clinical and immunologic evaluation of 31 patients with acute schistosomiasis mansoni. J Infect Dis. 2002; 185:98–105. [PubMed: 11756987]

7. Burke ML, Jones MK, Gobert GN, Li YS, Ellis MK, McManus DP. Immunopathogenesis of human schistosomiasis. Parasite Immunol. 2009; 31:163–176. [PubMed: 19292768]
8. Kaviratne M, Hesse M, Leusink M, Cheever AW, Davies SJ, McKerrow JH, Wakefield LM, Letterio JJ, Wynn TA. IL-13 activates a mechanism of tissue fibrosis that is completely TGF-beta independent. J Immunol. 2004; 173:4020–4029. [PubMed: 15356151]
9. Graham BB, Mentink-Kane MM, El-Haddad H, Purnell S, Zhang L, Zaiman A, Redente EF, Riches DW, Hassoun PM, Bandeira A, Champion HC, Butrous G, Wynn TA, Tuder RM. Schistosomiasis-induced experimental pulmonary hypertension: role of interleukin-13 signaling. Am J Pathol. 2010; 177:1549–1561. [PubMed: 20671265]
10. Jenkins SJ, Ruckerl D, Cook PC, Jones LH, Finkelman FD, van RN, MacDonald AS, Allen JE. Local macrophage proliferation, rather than recruitment from the blood, is a signature of TH2 inflammation. Science. 2011; 332:1284–1288. [PubMed: 21566158]
11. Montani D, Perros F, Gambaryan N, Girerd B, Dorfmuller P, Price LC, Huertas A, Hammad H, Lambrecht B, Simonneau G, Launay JM, Cohen-Kaminsky S, Humbert M. C-kit-positive cells accumulate in remodeled vessels of idiopathic pulmonary arterial hypertension. Am J Respir Crit Care Med. 2011; 184:116–123. [PubMed: 21471108]
12. Varghese AJ, Gulyas S, Mohindra JK. Hypoxia-dependent reduction of 1-(2-nitro-1-imidazolyl)-3-methoxy-2-propanol by Chinese hamster ovary cells and KHT tumor cells in vitro and in vivo. Cancer Res. 1976; 36:3761–3765. [PubMed: 986241]
13. Daley E, Emson C, Guignabert C, de Waal MR, Louten J, Kurup VP, Hogaboam C, Taraseviciene-Stewart L, Voelkel NF, Rabinovitch M, Grunig E, Grunig G. Pulmonary arterial remodeling induced by a Th2 immune response. J Exp Med. 2008; 205:361–372. [PubMed: 18227220]
14. Nomura M, Li E. Smad2 role in mesoderm formation, left-right patterning and craniofacial development. Nature. 1998; 393:786–790. [PubMed: 9655392]
15. Richter A, Yeager ME, Zaiman A, Cool CD, Voelkel NF, Tuder RM. Impaired transforming growth factor-beta signaling in idiopathic pulmonary arterial hypertension. Am J Respir Crit Care Med. 2004; 170:1340–1348. [PubMed: 15361368]
16. Lane KB, Machado RD, Pauciulo MW, Thomson JR, Phillips JA III, Loyd JE, Nichols WC, Trembath RC. Heterozygous germline mutations in BMPR2, encoding a TGF-beta receptor, cause familial primary pulmonary hypertension. Nat Genet. 2000; 26:81–84. [PubMed: 10973254]
17. Crosby A, Soon E, Jones F, Southwood M, Dunmore B, Dunne D, Morrell NW. Bmpr-ii deficiency does not worsen pulmonary arterial hypertension in the mouse model of chronic schistosomiasis infection. Am J Respir Crit Care Med. 2012; 185:A3438.
18. Ma W, Han W, Greer PA, Tuder RM, Toque HA, Wang KK, Caldwell RW, Su Y. Calpain mediates pulmonary vascular remodeling in rodent models of pulmonary hypertension, and its inhibition attenuates pathologic features of disease. J Clin Invest. 2011; 121:4548–4566. [PubMed: 22005303]
19. Zaiman AL, Podowski M, Medicherla S, Gordy K, Xu F, Zhen L, Shimoda LA, Neptune E, Higgins L, Murphy A, Chakravarty S, Protter A, Sehgal PB, Champion HC, Tuder RM. Role of the TGF-beta/Alk5 signaling pathway in monocrotaline-induced pulmonary hypertension. Am J Respir Crit Care Med. 2008; 177:896–905. [PubMed: 18202349]
20. Dorfmuller P, Perros F, Balabanian K, Humbert M. Inflammation in pulmonary arterial hypertension. European Resp J. 2003; 22:358–363.
21. Nagaoka T, Morio Y, Casanova N, Bauer N, Gebb S, McMurtry I, Oka M. Rho/Rho kinase signaling mediates increased basal pulmonary vascular tone in chronically hypoxic rats. Am J Physiol Lung Cell Mol Physiol. 2004; 287:L665–L672. [PubMed: 12959926]
22. Oka M, Homma N, Taraseviciene-Stewart L, Morris KG, Kraskauskas D, Burns N, Voelkel NF, McMurtry IF. Rho kinase-mediated vasoconstriction is important in severe occlusive pulmonary arterial hypertension in rats. Circ Res. 2007; 100:923–929. [PubMed: 17332430]
23. Japyassu FA, Mendes AA, Bandeira AP, Oliveira FR, Sobral FD. Hemodynamic profile of severity at pulmonary vasoreactivity test in schistosomiasis patients. Arq Bras Cardiol. 2012; 99:789–796. [PubMed: 22836358]
24. Hoot KE, Lighthall J, Han G, Lu SL, Li A, Ju W, Kulesz-Martin M, Bottinger E, Wang XJ. Keratinocyte-specific Smad2 ablation results in increased epithelial-mesenchymal transition

during skin cancer formation and progression. J Clin Invest. 2008; 118:2722–2732. [PubMed: 18618014]

25. Shadan S. Drug discovery: schistosome treatment. Nature. 2008; 452:296. [PubMed: 18354470]
26. Steinmann P, Keiser J, Bos R, Tanner M, Utzinger J. Schistosomiasis and water resources development: systematic review, meta-analysis, and estimates of people at risk. Lancet Infect Dis 2006 Jul. 2006:411–425.
27. Oh CK, Geba GP, Molfino N. Investigational therapeutics targeting the IL-4/IL-13/STAT-6 pathway for the treatment of asthma. Eur Respir Rev. 2010; 19:46–54. [PubMed: 20956165]

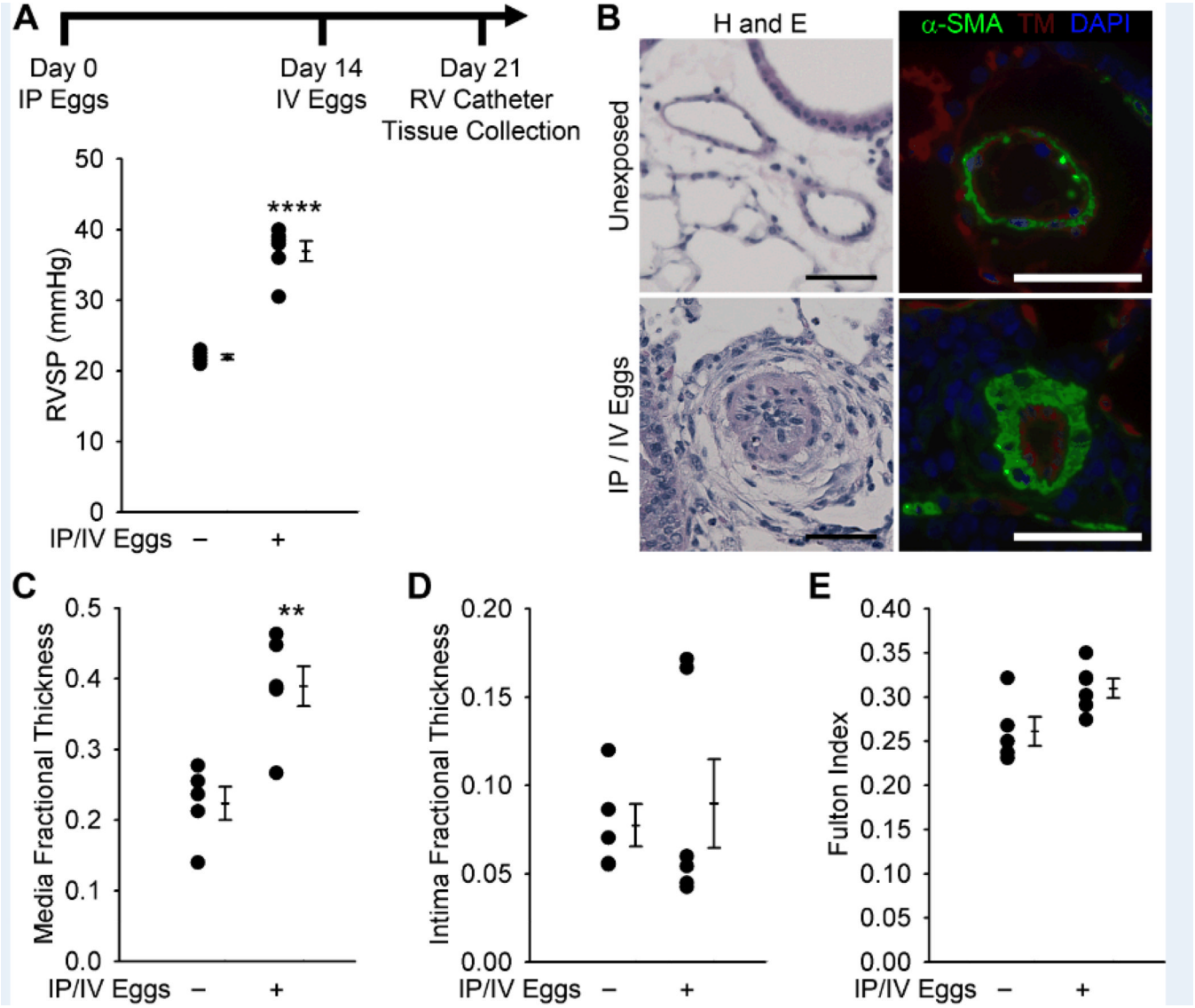

Figure 1.

Mice exposed to *S. mansoni* eggs develop PH and vascular remodeling. (**A**) Mice IP sensitized to *S. mansoni* eggs followed by IV augmentation have an increase in RVSP (mean ± SE; n = 5–6 mice per group; rank-sum test ****P < 0.001; this experiment was repeated 3 times with similar results). (**B**) Representative H&E and immunofluorescence staining for α-smooth muscle actin (α-SMA) and thrombomodulin of unexposed and IP/IV egg exposed mouse lungs (Scale bars: 50μm). (**C** and **D**) Quantitative fractional thickness of the pulmonary vascular media and intima in unexposed and IP/IV egg-exposed mice (mean ± SE; n = 5–6 mice per group; rank-sum test **$P < 0.01$; P=0.66 for intima thickness). (**E**) Fulton index (RV/(LV+S)) of unexposed and IP/IV egg exposed mice (mean ± SE; n = 5–6 mice per group; rank-sum test $P = 0.052$).

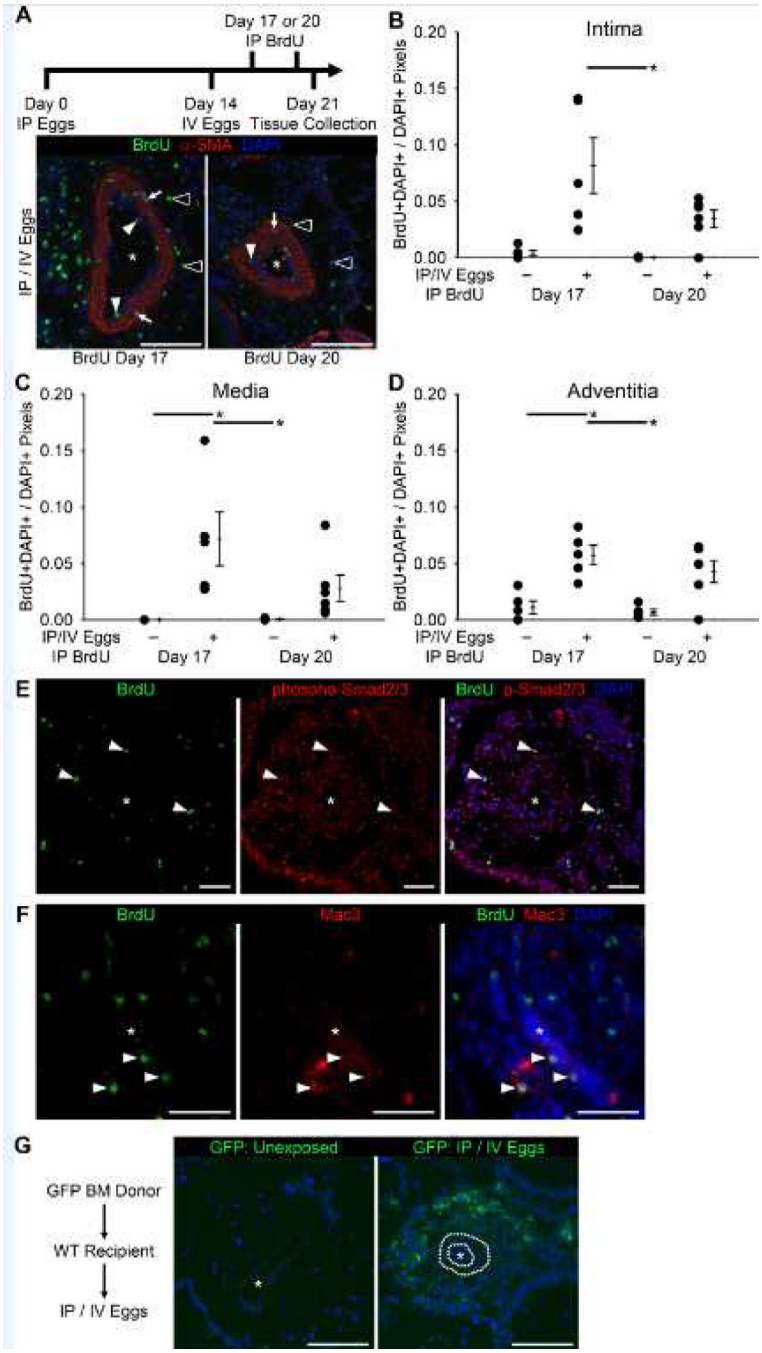

Figure 2.

There is pulmonary vascular proliferation in *S. mansoni* egg exposed mice, with an adventitial bone marrow-derived infiltrate. (**A**) Tissue from mice exposed to BrdU at the indicated timepoints, stained for α-smooth muscle actin (α-SMA) and BrdU (* vascular lumen; white arrowheads: BrdU+ intima cells; white arrows: BrdU+ media cells; outlined arrowheads: BrdU+ adventitia cells; Scale bars: 100μm). (**B**–**D**) Quantified fraction of cell nuclei BrdU+ in the intima, media and adventitia compartments (mean ± SE; n = 5–6 mice per group; ANOVA on ranks P=0.004 for intima, P<0.001 for media, and P=0.010 for adventitia; *P < 0.05 by post-hoc Dunn's test). (**E**) Co-localization of BrdU and phospho-

Smad2/3 positive cells (* vascular lumen; Scale bars: 50μm). (**F**) Co-localization of BrdU and Mac3 positive cells (macrophages; * vascular lumen; Scale bars: 50μm). (**G**) GFP signal in wildtype recipient mice with GFP positive bone marrow donor (* vascular lumen; dotted line in IP/IV image mark the inner and outer elastic laminae; Scale bars: 100μm; same image without dotted lines is in Figure S5B).

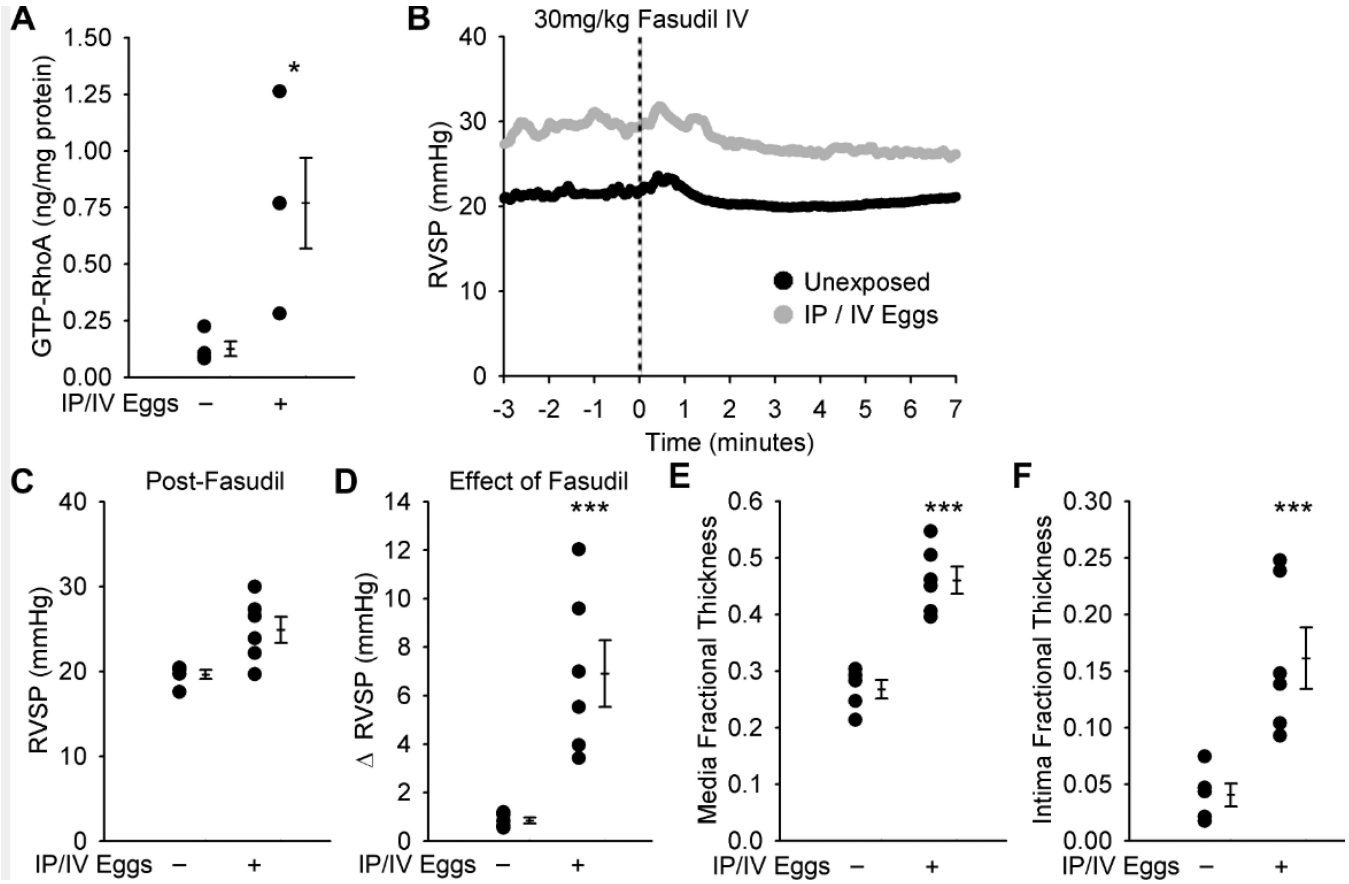

Figure 3.

The Rho kinase inhibitor fasudil acutely decreases but does not normalize the RVSP in IP/IV *S. mansoni* egg-exposed mice. (**A**) GTP-bound (active) RhoA concentration in unexposed and egg exposed mice (mean ± SE; n = 4 mice per group; rank-sum test **P* < 0.05). (**B**) Representative plots of the effect of fasudil on RVSP in unexposed and egg exposed mice (N=1 per group), administered at time = 0. (**C** and **D**) RVSP in unexposed and IP/IV egg exposed mice 5 minutes after fasudil administration, and the decrease in pressure with fasudil treatment (mean ± SE; n = 5–6 mice per group; rank-sum test *P* = 0.052 for post-fasudil; ****P* < 0.005). (**E** and **F**) Quantitative fractional thickness of the pulmonary vascular media and intima in unexposed and egg exposed mice after fasudil administration (mean ± SE; n = 5–6 mice per group; rank-sum test ****P* < 0.005).

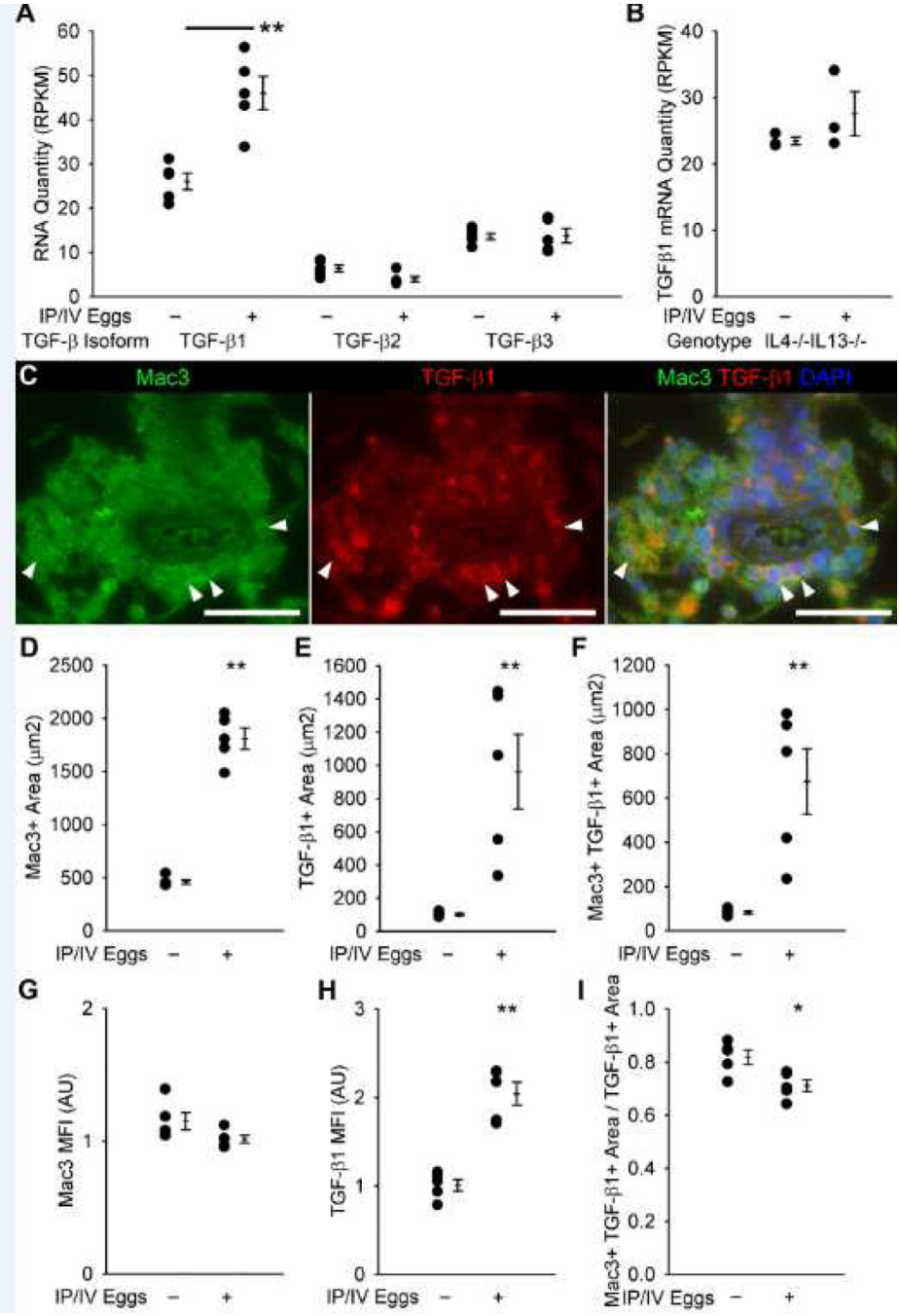

Figure 4.

TGF-β mRNA expression and protein co-localization with antibodies targeting Mac3 (a macrophage marker). (**A**) TGF-β1, 2 and 3 isoform mRNA quantities in wildtype unexposed and egg-exposed mice (RPKM: reads per kilobase of exon model per million mapped reads; mean ± SE; n = 5 mice per group; rank-sum test ***P*<0.01). (**B**) TGF-β1 mRNA quantities in IL4−/−IL13−/− unexposed and egg-exposed mice (mean ± SE; n = 3 mice per group; rank-sum test *P*=0.20). (**C**) Representative images showing Mac3 and TGF-β1 co-localization in the adventitia of an IP/IV *S. mansoni* egg-exposed mouse (Arrowheads mark double-positive cells; Scale bars: 50 μm). (**D**–**F**) Quantification of Mac3+, TGF-β1+, and

Mac3+ and TGF-β1+ co-localized areas in the adventitia (mean ± SE; n = 5 mice per group; rank-sum test $^{**}P<0.01$). (**G**–**H**) Mean fluorescent intensity of Mac3+ and TGF-β1+ pixels (arbitrary units; normalized to average of uninfected adventitia = 1; mean ± SE; n = 5 mice per group; rank-sum test $^{**}P<0.01$; $P=0.056$ for Mac3 intensity). (**I**) Ratio of co-localized Mac3+ and TGF-β1+ area to all TGF-β1+ area in the adventitia (mean ± SE; n = 5 mice per group; rank-sum test $^{*}P<0.05$).

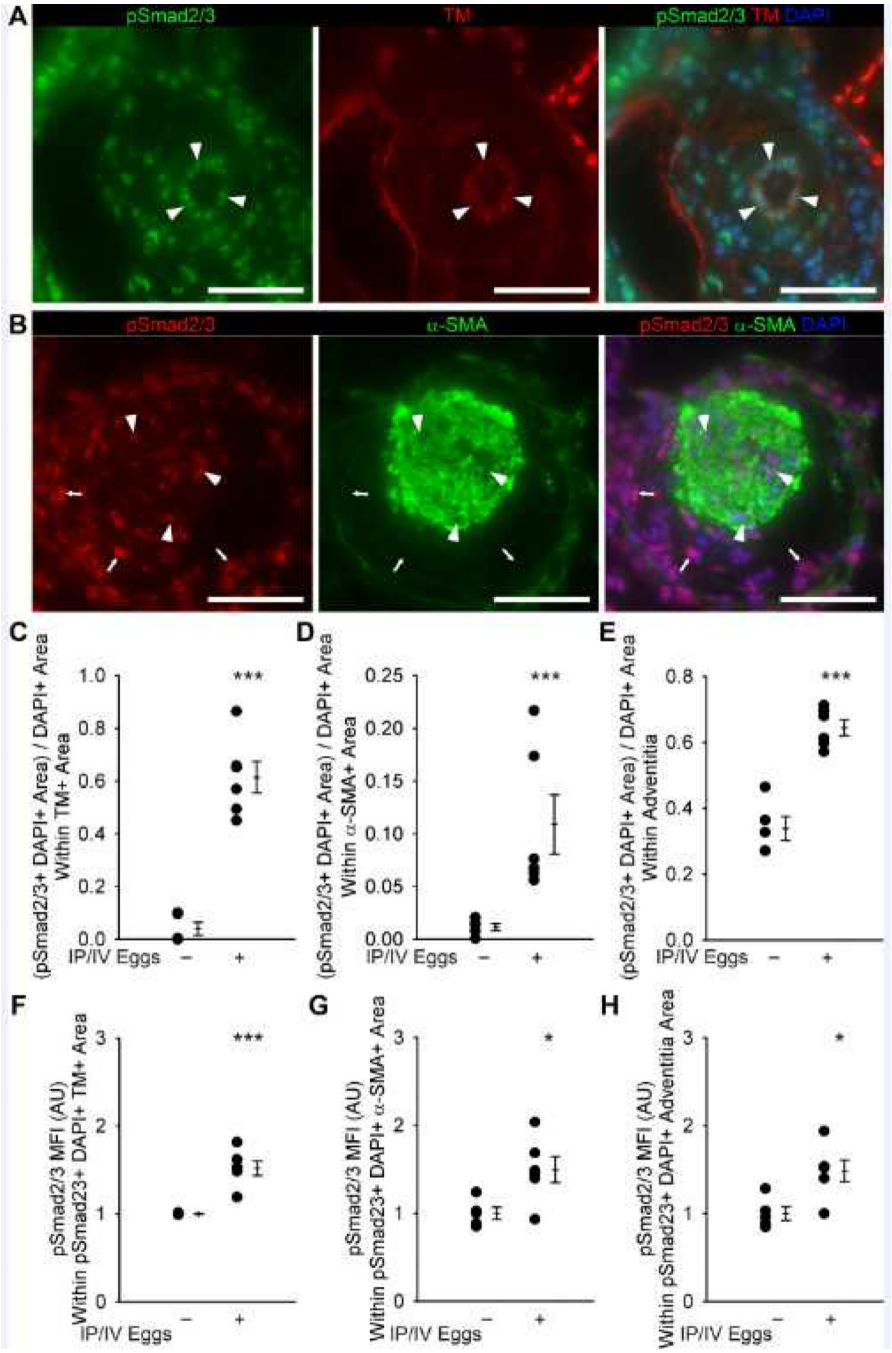

Figure 5.

Quantification of phospho-Smad2/3 and co-localization with vascular compartments in unexposed and mice exposed to IP/IV *S. mansoni* eggs. (**A**) Representative images showing phospho-Smad2/3 and thrombomodulin (TM) co-localization in the intima of an egg-exposed mouse (arrowheads mark double-positive cells; Scale bars: 50 μm). (**B**) Representative images showing phospho-Smad2/3 and α-smooth muscle actin (α-SMA) co-localization in the media, and identifying the adventitia, of an IP/IV *S. mansoni* egg-exposed mouse (arrowheads mark double-positive cells in the media; arrows mark phospho-Smad2/3+ cells in the adventitia; Scale bars: 50 μm). (**C**–**E**) Quantification of phospho-

Smad2/3+ thrombomodulin+ area in the intima, media and adventitia (mean ± SE; n = 5–6 mice per group; rank-sum test ***P<0.005). (**F**–**H**) Mean fluorescent intensity of phospho-Smad2/3+ pixels in the initima, media and adventitia (arbitrary units; normalized to average of uninfected = 1; mean ± SE; n = 5–6 mice per group; rank-sum test *P<0.05, ***P<0.005).

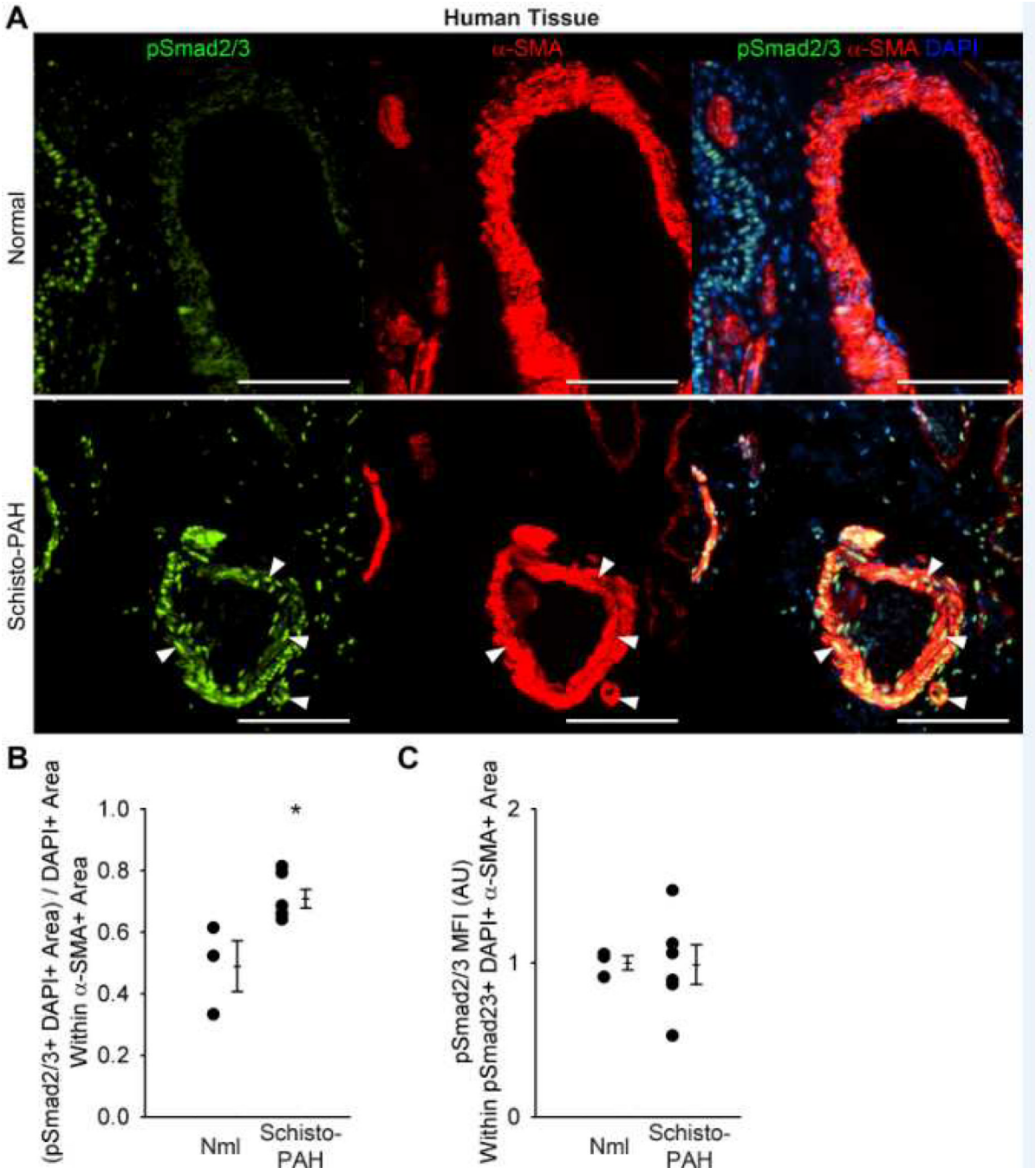

Figure 6.

Human schistosomiasis-PAH tissue analysis by phospho-Smad2/3 quantification and co-localization with the media vascular compartment, as compared to control tissue from failed lung donors. (**A**) Representative images showing phospho-Smad2/3 and α-smooth muscle actin (α-SMA) co-localization in the media of normal control and Sc-PAH cases (arrowheads mark double-positive cells; Scale bars: 100 μm). (**B**) Quantification of phospho-Smad2/3 α-SMA double-positive area in the media (mean ± SE; n = 3–6 cases per group; rank-sum test *P<0.05). (**C**) Mean fluorescent intensity of phospho-Smad2/3+ pixels

in the media (arbitrary units; normalized to average of control = 1; mean ± SE; n = 3–6 cases per group; rank-sum test P=1.0).

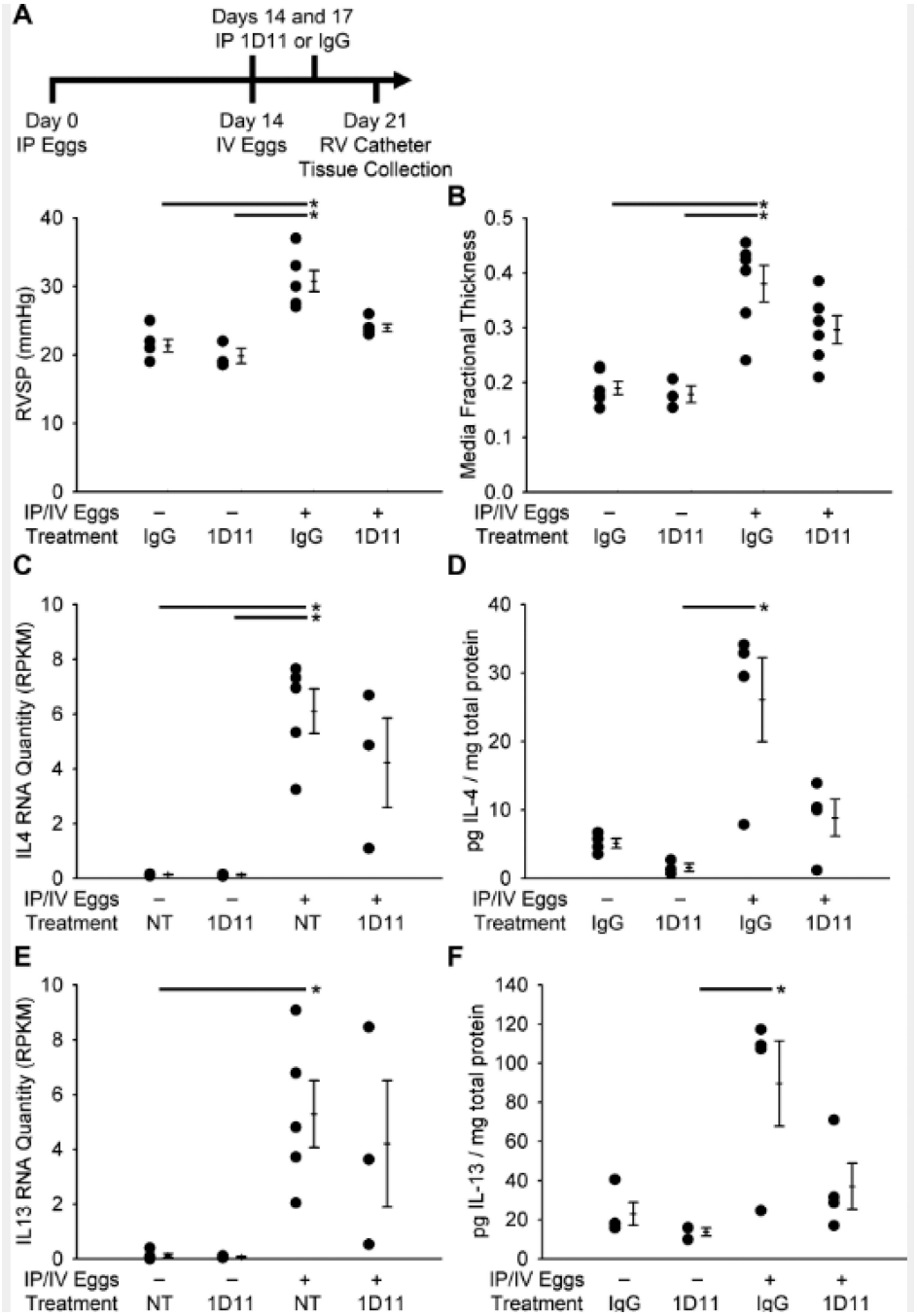

Figure 7.

Treatment with the pan-TGF-β neutralizing antibody 1D11 prevents the increase in pressure from IP/IV *S. mansoni* egg exposure. (**A**) RVSP in mice treated with 1D11 or IgG control, and unexposed or exposed to eggs (mean ± SE; n = 3–6 mice per group; ANOVA on ranks P=0.001; *P < 0.05; by post-hoc Dunn's test). (**B**) Quantitative fractional thickness of the pulmonary vascular media in mice treated with 1D11 or IgG control, and unexposed or egg exposed (mean ± SE; n = 3–6 mice per group; ANOVA on ranks P=0.002; *P < 0.05 by post-hoc Dunn's test). (**C**–**F**) IL4 and IL13 RNA and protein quantity as measured by RNA-seq and ELISA in mice treated with 1D11, IgG, or no treatment (NT), unexposed or IP/IV

exposed to *S. mansoni* eggs (RPKM: reads per kilobase of exon model per million mapped reads; mean ± SE; n = 3–5 mice per group; ANOVA on ranks P=0.008 for IL4 RNA data, P=0.025 for IL4 protein data, P=0.010 for IL13 RNA data, P=0.027 for IL13 protein data; *P<0.05 by post-hoc Dunn's test).

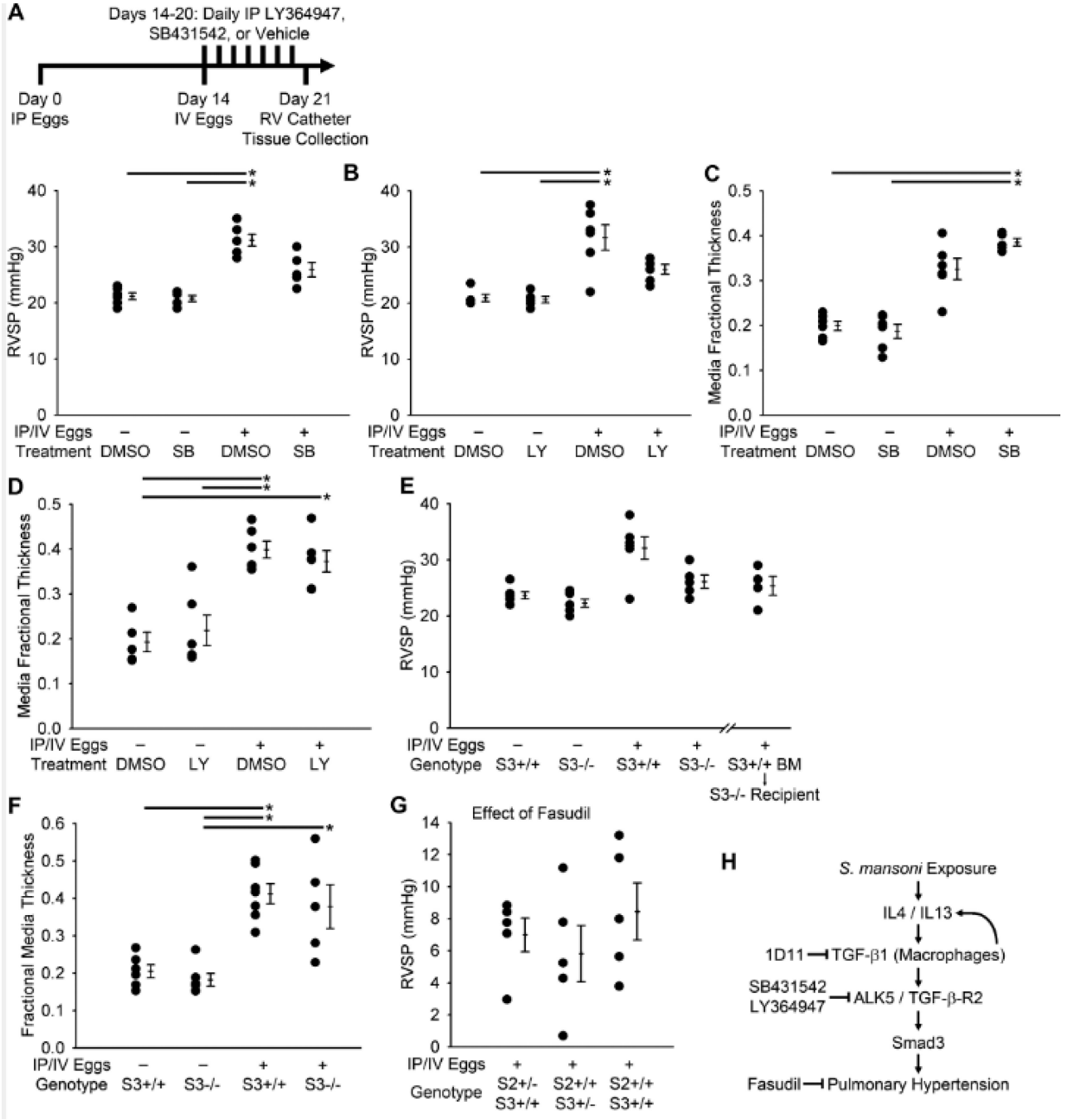

Figure 8.

Treatment with either of two ALK5 inhibitors prevents the increase in pressure from IP/IV *S. mansoni* egg exposure, as does Smad3−/− genotype, specifically in peripheral tissue. (**A**–**B**) RVSP in mice treated with SB431542, LY364947, or DMSO vehicle, and unexposed or egg exposed (mean ± SE; n = 5–6 mice per group; ANOVA on ranks $P<0.001$ for SB431542, P=0.002 for LY364947; *$P < 0.05$ by post-hoc Dunn's test). (**C**-**D**) Quantitative fractional thickness of the pulmonary vascular media in mice treated with SB431542, LY364947, or DMSO vehicle, and unexposed or egg exposed (mean ± SE; n = 5–6 mice per group; ANOVA on ranks $P<0.001$ for SB431542, $P=0.002$ for LY364947; *$P < 0.05$ by

post-hoc Dunn's test). (**E**) RVSP in Smad3+/+ and Smad3−/− mice, and Smad3−/− mice who were lethally irradiated and received Smad3+/+ bone marrow cells, unexposed or egg exposed (mean ± SE; n = 4–7 mice per group; ANOVA on ranks P=0.035). (**F**) Quantitative fractional thickness of the pulmonary vascular media in Smad3+/+ and Smad3−/− mice unexposed or egg exposed (mean ± SE; n = 5–7 mice per group; ANOVA on ranks P<0.001; *P < 0.05 by post-hoc Dunn's test). (**G**) Decrease in RVSP by acute administration of the Rho kinase inhibitor fasudil in mice lacking Smad2 and/or Smad3 (mean ± SE; n = 5–6 mice per group; ANOVA on ranks P=0.53). (**H**) Proposed signaling outline linking *S. mansoni* exposure with pulmonary hypertension.